

The Influence of Aggregation on Triplet Formation in Light-Harvesting Chlorophyll *a/b* Pigment–Protein Complex II of Green Plants[†]

Virginijus Barzda,* Erwin J. G. Peterman, Rienk van Grondelle, and Herbert van Amerongen

Department of Physics and Astronomy and Institute for Molecular Biological Sciences, Vrije Universiteit, De Boelelaan 1081, 1081 HV Amsterdam, The Netherlands

Received August 26, 1997; Revised Manuscript Received October 29, 1997[⊗]

ABSTRACT: The influence of aggregation on triplet formation in the light-harvesting pigment–protein complex of photosystem II of green plants (LHCII) has been studied with time-resolved laser flash photolysis. The aggregation state of LHCII has been varied by changing the detergent concentration. The triplet yield increases upon disaggregation and follows the same dependence on the detergent concentration as the fluorescence yield. The rate constant of intersystem crossing is not altered by disaggregation, and variations of the triplet yield appear to be due to aggregation-dependent quenching of singlet excited states. The efficiency of triplet transfer in LHCII aggregates from chlorophyll (Chl) to carotenoid (Car) is $92 \pm 7\%$ at room temperature and $82 \pm 6\%$ at 5 K, and does not change upon disaggregation. The Chl's that do not transfer their triplets to Car's seem to be bound to LHCII and are capable of transferring/accepting their singlet excitations to/from other Chl's. Two spectral contributions of Car triplets are observed: at 525 and 506 nm. Disaggregation of macroaggregates to small aggregates reduces by 10% the relative contribution of Car triplets absorbing at 525 nm. This effect most likely originates from a decreased efficiency of intertrimer Chl-to-Car triplet transfer. At the critical micelle concentration, at which small aggregates are disassembled into trimers, the interactions between Chl and Car are changed. At room temperature, this effect is much more pronounced than at 5 K.

A high degree of organization of pigments in pigment–protein complexes is required for efficient utilization of solar energy in photosynthetic organisms (1). Besides chlorophylls (Chl's),¹ the major light-harvesting pigment–protein complex of photosystem II (LHCII) of green plants contains carotenoids (Car's) which are in close contacts with Chl molecules, as revealed by the crystal structure (2). Three roles for Car have been proposed: (i) A role in light-harvesting: absorption of light is followed by singlet–singlet energy transfer from Car to Chl, which increases the efficiency of collection of solar energy in the wavelength region where Chl does not absorb (3). (ii) A structural role: reconstituted LHCII cannot be formed without Car molecules (4). (iii) A protecting role: triplet–triplet energy transfer from Chl to Car prevents the sensitization of singlet oxygen by Chl triplets (3).

Pigment analysis has shown that LHCII contains three types of Car's: two lutein, one neoxanthin, and less than one violaxanthin per monomer of LHCII (5, 6). Only two Car molecules have been resolved in the crystal structure

(2) and were assigned to lutein. These Car's are located in the center of the complex and are in close contacts to several Chl molecules.

LHCII mediates stacking of thylakoid membranes (7). Isolated LHCII readily forms macroaggregates in a detergent-free medium or after the addition of monovalent or bivalent ions to the suspension containing detergents in concentrations which are below the critical micelle concentration (CMC) (8, 9). Disaggregation induces changes in the spectroscopic properties of LHCII. Large CD signals gradually decrease and the fluorescence quantum yield increases upon disaggregation of macroaggregates into small aggregates (10–12). The main (severalfold) increase of the fluorescence yield appears at the CMC of the detergent when small aggregates are disassembled into trimers (12). At the CMC changes in the absorbance, CD and LD are observed, both in the Car and in the Chl *a* Q_y absorption region (13; Barzda et al., unpublished results). ADMR (absorbance-detected magnetic resonance), FDMR (fluorescence-detected magnetic resonance), and laser flash photolysis measurements revealed specific interactions between Car and Chl molecules and the influence of LHCII oligomerization on triplet formation on different Car's (6, 14, 15). These observations stimulated a further study of the influence of aggregation on interactions between Chl and Car in LHCII. The results of laser flash photolysis investigations are presented in this article.

Chl and Car triplets in LHCII were characterized by laser flash photolysis (6, 16), EPR (17), ADMR (14, 18) and FDMR (15, 19) techniques. It has been shown that the

[†] This work was supported by the Netherlands Foundation for Scientific Research (NWO) via the Foundation for Life Sciences (SLW). V.B. was supported by EMBO Fellowship ALTF 131-1996.

* To whom correspondence should be addressed. Telephone: +31-20-444-7934. Fax: +31-20-444-7899. E-mail: virgis@nat.vu.nl.

[⊗] Abstract published in *Advance ACS Abstracts*, December 15, 1997.

¹ Abbreviations: LHCII, light-harvesting chlorophyll *a/b* pigment–protein complex of photosystem II; Chl, chlorophyll; Car, carotenoid; CMC, critical micelle concentration; ADMR, absorbance-detected magnetic resonance; FDMR, fluorescence-detected magnetic resonance; DM, *n*-dodecyl β -D-maltoside; TX-100, TRITON X-100; T–S, triplet minus singlet; LD, linear dichroism; CD, circular dichroism.

efficiency of Chl triplet transfer to Car is close to 100% at room temperature (6). The lifetime of Car triplets under anaerobic conditions is 9 μ s (6) whereas the Chl *a* triplet lifetime is of the order of milliseconds.

Three Car triplets have been distinguished with ADMR measurements: one with a $|D|+|E|$ transition at 1273 MHz and T–S absorption peaks near 507 and 525 nm, and two other triplets having $|D|+|E|$ transitions at 1303 and 1322 MHz and corresponding to an absorption maximum at 525 nm (14). These triplets were assigned to the three different Car species present in the LHCII complex. Signals decaying with a 9 μ s lifetime (Car triplet lifetime) at room temperature were also found in the Q_y absorption region of Chl *a* (6). These signals were attributed to strong interactions between Chl and Car (6). It was also observed by ADMR and FDMR that at the $|D|+|E|$ transition the ratio of the magnitude of the Car triplet signals leading to absorption at 507 and 525 nm is changing by varying the concentration of LHCII in the sample (14, 15), whereas the $2|E|$ transition was not affected. This observation was ascribed to enhanced population of specific Car triplets absorbing at 525 nm due to oligomerization of LHCII and the appearance of “inter-trimer” transfer of triplets.

In the present study, Car and Chl triplet formation for different aggregation states of LHCII was investigated by laser flash photolysis. We found that the rate constant of intersystem crossing was not influenced by aggregation. The rate of triplet transfer from Chl's to Car's was enhanced only a few percent by aggregation. The major effect, aggregation-dependent changes in the yield of triplets, appeared to be due to changes in the quenching of singlet excited states.

EXPERIMENTAL PROCEDURES

Stacked lamellar aggregates of LHCII were isolated as described in (9). Disaggregation of LHCII macroaggregates was achieved by adding *n*-dodecyl β -D-maltoside (DM) or TRITON X-100 (TX-100). The state of aggregation was monitored with CD and fluorescence measurements (11, 12). The fluorescence yield was measured with a CCD camera by exciting the sample in the Soret region with low-intensity light in order to avoid exciton annihilation effects. Laser photolysis measurements were performed using a 1 cm \times 1 cm cuvette. The sample concentration was 15 μ g/mL Chl, which corresponds to an optical density of 0.7 at 680 nm (for aggregates). Anaerobic conditions were obtained by degassing the sample under reduced pressure and flushing it subsequently with argon. During laser flash photolysis measurements at room temperature, degradation of the sample was observed when detergent concentrations far above the CMC were used [$>0.03\%$ (v/v) for TX-100 or $>0.06\%$ (w/v) for DM; the CMC for TX-100 and DM is ca. 0.015% (v/v) and 0.009% (w/v), respectively]. Thus, all measurements were performed at lower detergent concentrations. For low-temperature measurements, the state of aggregation was adjusted by adding the detergent first and then diluting the sample with glycerol containing the same amount of detergent. A glycerol concentration of 65% (v/v) was used for low-temperature measurements. The addition of glycerol slightly shifted the CMC transition to 0.018% for TX-100 and to 0.013% for DM. Low-temperature measurements were performed in a helium bath cryostat (Utreks).

Laser flash-induced triplet minus singlet (T–S) absorption difference measurements were performed on the setup described earlier (6, 20). Excitation pulses (~ 8 ns full width at half-maximum, ~ 10 mJ) from a dye laser at 590 nm (dye: Rhodamine 610) pumped by a frequency-doubled Nd:YAG laser (Quanta Ray DCR2) were used. 20 ms pulses of measuring light were obtained from a 450 W Xenon lamp in combination with a shutter. The measuring light was filtered to obtain the appropriate wavelength for the measuring beam and to minimize heating and actinic effects. The transmitted light was detected via a 1/4 m monochromator with a photomultiplier (Hamamatsu R928). The repetition rate of the setup was 2 Hz, and the instrument response time was less than 0.5 μ s. Kinetic traces were averaged 128 or 256 times on a digital oscilloscope preceding the transfer to the computer for data analysis. T–S decay-associated spectra were constructed from global analysis of the decay kinetics recorded at different wavelengths (21). A model with two exponential decays was needed to fit the T–S measurements at room temperature, and a three-exponential model was used to fit the 5 K measurements [see also (6)]. The quality of the fits was evaluated by global χ^2 values, plots of residuals, and Studentised residuals (21). The relative triplet yield under exciton–exciton annihilation free conditions (22) was estimated from the slope at zero intensity of saturation curves of T–S signals recorded at the maximum of the Car triplet absorption (~ 508 nm) (23). The Chl-to-Car triplet transfer efficiency was estimated by dividing the amount of Car triplets by the total amount of triplets on both Chl and Car. The amount of triplets was estimated by the area under the triplet absorption bands determined from the global analysis: for Chl the negative bands in the Q_y region between 660 and 700 nm, and for Car the positive bands between 500 and 550 nm. Extinction coefficients of 1×10^5 M $^{-1}$ cm $^{-1}$ for Chl *a* at 670–680 nm and 2.4×10^5 M $^{-1}$ cm $^{-1}$ for Car in the 500–540 nm region were used as in (6). It was assumed that the ratio between the two extinction coefficients was proportional to the ratio between the areas under the absorption bands.

RESULTS

Room Temperature Measurements. Room temperature laser photolysis measurements on LHCII at different aggregation states were performed under anaerobic conditions. Global analysis of the T–S kinetics recorded at different wavelengths revealed two decay-associated spectral components: a Car component with a lifetime of 9 μ s and a Chl component with a lifetime in the millisecond range [see also (6)]. T–S kinetics were recorded up to 100 μ s; thus, the lifetime of the Chl component was not accurately resolved. The lifetime of the Car component did not depend on the state of aggregation. Figure 1 shows room temperature T–S spectra of the Car component of LHCII macroaggregates, small aggregates, and trimers, as obtained by global analysis. Spectra were normalized to the maximum near 508 nm. The spectra are very similar to the spectra of LHCII trimers reported earlier (6). Disaggregation leads to a blue shift of the T–S band around 508 nm and a small relative decrease of the shoulder of the Car triplet absorption around 525 nm as compared to the peak at 508 nm. The shift of the peak from 508 to 506 nm can be explained by the relative decrease of the contribution of the Car with its maximum near 525

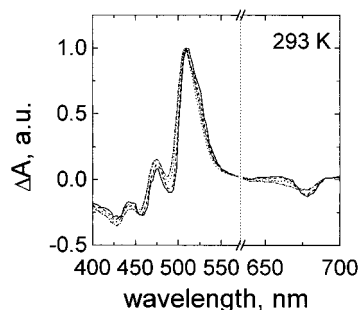


FIGURE 1: Room temperature T-S decay-associated spectra of the Car component (the $9 \mu\text{s}$ component as determined from global analysis) of macroaggregates (solid line, 0% of TX-100), small aggregates (dashed line, 0.01%), trimers (dotted line, 0.02%), and trimers (uneven dashed line, 0.03%) of LHCII. The spectra were normalized to the 508 nm peak. The spectra in mOD can be obtained by multiplication with 8.3, 14, 27, and 31.2 going from macroaggregates to trimers. No spectral points were measured between 550 and 640 nm.

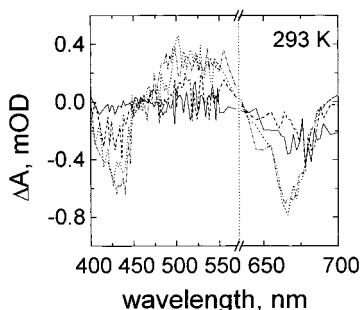


FIGURE 2: Room temperature T-S decay-associated spectra of the Chl component (determined as a millisecond component from the global analysis) at different aggregation states of LHCII. The same line symbols and the same spectral ranges were used as in Figure 1.

nm, which has a negative peak near 510 nm due to the ground state bleaching (24). Upon oligomerization, large changes in the ratio of the T-S signals at 525 and 507 nm were previously observed, probing the $|D\rangle+|E\rangle$ transition with ADMR (14). Disaggregation-induced changes show that different Car's are populated by the triplets giving rise to absorption at 525 and 508 nm. It is interesting to note that signals decaying with the lifetime of Car triplets are present in the Chl Q_y region around 678 nm. These signals decrease relative to the signals in the Car triplet absorption region around 508 nm upon disaggregation. Previously, these signals were observed in T-S spectra of trimers (6).

The millisecond components of T-S decay-associated spectra of LHCII macroaggregates, small aggregates, and trimers are shown in Figure 2. These signals are about 40 times smaller than the Car signals, but the characteristic features of T-S spectra of Chl a molecules (bleaching near 435 and 670 nm) can be distinguished. The overall amplitudes of both kinetic components (Car and Chl) of the T-S signals increase upon disaggregation and follow a similar dependence on the detergent concentration (compare Figures 1 and 2). Thus, the efficiency of Chl to Car triplet transfer remains largely unchanged and is $92 \pm 7\%$. The large error margins in the efficiency arise due to a very low signal to noise ratio in T-S spectra of Chl and uncertainties in determination of the area under the Car triplet absorption band due to overlap with the negative band of ground state bleaching (6).

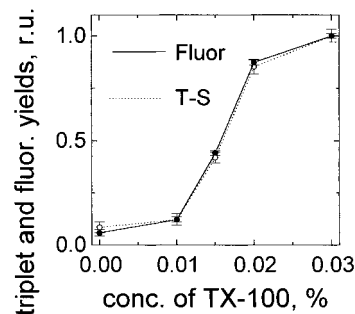


FIGURE 3: Comparison of the relative triplet yield and the relative fluorescence yield at different aggregation states of LHCII. (Determination methods are described under Experimental Procedures.)

The increase in the total amplitudes of the triplet signals upon disaggregation might be due to a change in the rate of intersystem crossing, but also to a change in the rate of competing processes like internal conversion. In order to obtain information on the exact cause of this effect, we have compared the Car triplet quantum yield at different detergent concentrations to the fluorescence quantum yield measured on the same samples. Both quantum yields are shown in Figure 3. The triplet yield and fluorescence quantum yields show a similar dependence on the aggregation state of LHCII. Both show a transition around the CMC with a substantial increase of the signals. The characteristic increase in the fluorescence yield at the CMC was observed and discussed previously (12).

5 K Measurements. In order to study disaggregation-induced spectral changes in more detail, we also performed the T-S measurements at 5 K. A global fit of the kinetics at different wavelengths requires three exponential decay times and three spectral components. One component has a decay time of several milliseconds and is due to Chl triplets. The other two correspond to Car triplets described by two different microsecond decay times. In zero magnetic field, the triplet level is split into three sublevels mainly due to the dipolar interaction between the two unpaired electrons. In contrast to room temperature, the three triplet sublevels are partly uncoupled at low temperature which may result in different decay times from each triplet sublevel. LHCII contains three types of Car's. Thus, possibly nine sublevels with different decay times constitute the T-S signal decay of Car's. The three different Car's can have different triplet absorption spectra, each of them having three exponential decay times. For a proper description of the data, we need two Car spectral components (decay-associated spectra) with different lifetimes, which probably represent an average of the possible contributions given above. Fitting with more lifetimes and spectral components does not improve the fit. The lifetimes and relative contributions of the spectral components are presented in Table 1. Disaggregation increases the lifetime of the slower Car decaying component from 26 to 32 μs and decreases its contribution as compared to that of the faster component. The lifetime of the faster component also seems to increase slightly. Since the changes are small and for instance the average lifetime remains almost unaltered, we are hesitant to draw any further conclusions from these changes at this stage.

T-S spectra of Car components at different aggregation states of LHCII are presented in Figure 4A. Each spectrum is the sum of the two Car components (i.e., the total Car

Table 1: Lifetimes and Relative Contributions of the Car Decay Components of LHCII at 5 K with Different Concentrations of DM^a

DM, % (w/v)	$\tau_1, \mu\text{s}$	$\tau_2, \mu\text{s}$	a_2/a_1
0.0	5.8 ± 0.2	26.7 ± 0.7	0.83 ± 0.03
0.01	5.6 ± 0.2	25.6 ± 0.5	0.81 ± 0.03
0.02	6.7 ± 0.1	33.9 ± 0.8	0.60 ± 0.02
0.03	6.8 ± 0.1	30.9 ± 0.7	0.60 ± 0.02
0.06	6.9 ± 0.1	33.6 ± 0.8	0.55 ± 0.01

^a Decays were fit globally with three exponentials. The longest decay component was fixed to 2 ms. The components a_1 and a_2 reflect the decay-associated amplitudes of the T-S signal at 506 nm.

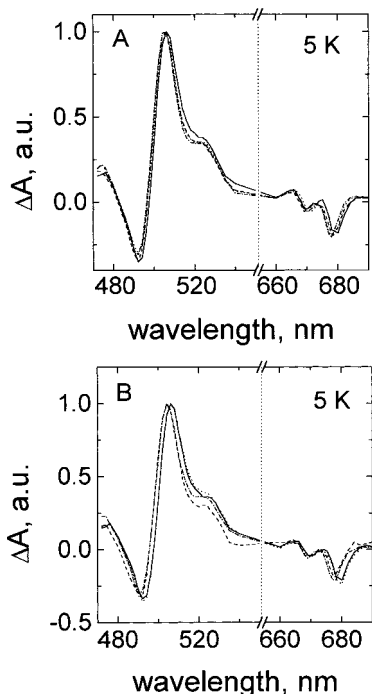


FIGURE 4: (A) Car T-S spectra at 5 K for macroaggregates (solid line, 0% DM), small aggregates (dashed line, 0.01% DM), trimers (dotted line, 0.02%; above CMC), and trimers (uneven dashed line, 0.03%; above CMC) of LHCII. Spectra were obtained by summing the two deconvoluted Car decay-associated spectral components and reflect the total Car T-S spectra before relaxation. The spectra were normalized at the 506 nm peak. The spectra in mOD can be obtained by multiplication with 6, 7.8, 12.4, and 13.8 going from macroaggregates to trimers. (B) T-S spectra of two deconvoluted Car spectral components decaying with 5.8 μs (solid line) and 26.7 μs (dotted line) for macroaggregates, and decaying with 5.6 μs (dashed line) and 25.6 μs (uneven dashed line) for small aggregates. The spectra were normalized to the 506 nm peak. Relative contributions of the spectra are presented in Table 1. No spectral points were measured between 540 and 660 nm.

T-S spectrum, the sum of the ~ 6 and the ~ 30 μs component). The spectra are normalized in the peak at 506 nm. Disaggregation leads to a $\sim 10\%$ decrease in the relative intensity of the 525 nm band. This shows that relatively more triplets are transferred to the Car's absorbing at 525 nm in the aggregates. The most significant change occurs between macroaggregates and small aggregates. We note that much larger differences were observed with ADMR upon oligomerization obtained by increasing the concentration of LHCII (14). In that case, the intensities depend on the differences in populations of the various sublevels, whereas in our case the sum of the populations on all three sublevels is measured. Both Car triplet components of macroaggregates and small aggregates are shown in Figure

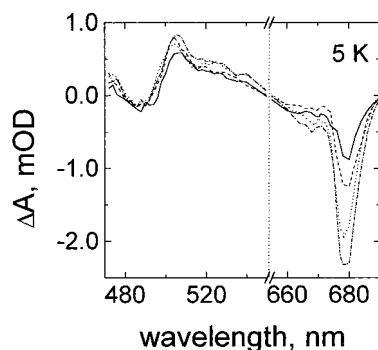


FIGURE 5: Low (5 K) temperature T-S decay-associated spectra of the millisecond component (predominantly Chl) at different aggregation states of LHCII. The same line symbols and the same spectral ranges were used as in Figure 4A.

4B. The main change that occurs is a relative decrease of the 525 nm band of the fast component upon going to small aggregates. The relative decrease of the 525 nm band of the fast component for small aggregates results in the decrease of this band in the sum of both components (Figure 4A). This effect shows that the population efficiency of Car triplet absorbing at 525 nm is changed during disassembly of macroaggregates to small aggregates. This might be due to a reduced intertrimer triplet transfer from Chl to Car: in the aggregate, some Chl's might be well connected to Car's in a neighboring trimer but worse within the same monomer. Spectra of both Car components of trimers (above CMC) appear to be comparable to the spectra of small aggregates (data not shown). Note that in all cases the faster component has relatively less intensity in the 525 nm band.

The T-S spectra of the millisecond component at different aggregation states of LHCII are presented in Figure 5. These are mainly due to Chl *a*, but a relatively small contribution from Car can be observed. The amplitude of the Chl T-S signal follows a similar aggregation dependence as the amplitude of the Car signal (compare amplitudes of Chl *a* bleaching at 680 nm in Figure 5 and multiplication factors in the figure legend of Figure 4). The main increase occurs around the CMC, similar as at room temperature.

DISCUSSION

Yield of Triplet Formation. Disaggregation induces an increase in the triplet yield. We have measured the Car triplet yield. Car triplets are formed with an efficiency independent of the aggregation state from Chl triplets, so we can use the Car triplet yield as a measure for the Chl triplet yield. The fluorescence yield also increases with the same dependence on the detergent concentration (Figure 3). The yield of triplet formation, Φ_{isc} , can be described as

$$\Phi_{\text{isc}} = k_{\text{isc}} / (k_{\text{f}} + k_{\text{isc}} + k_{\text{ic}}) \quad (1)$$

where k_{isc} , k_{f} , and k_{ic} are the rate constants of intersystem crossing, radiation, and internal conversion, respectively. The fluorescence yield, Φ_{f} , can be written as

$$\Phi_{\text{f}} = k_{\text{f}} / (k_{\text{f}} + k_{\text{isc}} + k_{\text{ic}}) \quad (2)$$

Since $\Phi_{\text{f}}/\Phi_{\text{isc}}$ is constant, it can be concluded that also $k_{\text{f}}/k_{\text{isc}}$ is constant upon disaggregation. The fact that both yields change in the same way strongly suggests that upon

disaggregation the denominator (which is the same in eq 1 and 2) changes whereas the nominators in eqs 1 and 2, i.e., k_{isc} and k_f remain constant. This implies that only k_{ic} changes upon disaggregation. This implication can be tested by comparing the results of fluorescence yield experiments and time-resolved fluorescence measurements. The denominator in eqs 1 and 2 is inversely proportional to the fluorescence lifetime. Therefore, the change in fluorescence yield is proportional to the fluorescence lifetime upon disaggregation if and only if the nominator in eq 2 (the radiative rate) remains constant. In a previous study, it was shown that the increase of Φ_f upon disaggregation is indeed proportional to the weighted sum of the observed fluorescence lifetimes (an interconversion of a 270 ps fluorescence lifetime to 3.5 ns component was observed around the CMC) (Barzda et al., unpublished results), demonstrating that the radiative rate is constant. Since k_f/k_{isc} also remains constant (see above), it is indeed confirmed that mainly k_{ic} decreases upon disaggregation. In conclusion: upon disaggregation, the radiative and intersystem crossing rates remain essentially unchanged. The increase in the triplet yield on both Chl and Car molecules can entirely be explained by a decrease of the quenching of singlet excited states. Apparently, the Chl's which do not transfer their triplets to Car's are still connected to the main bulk of Chl's via singlet excitation energy transfer.

Chl to Car Triplet Transfer Efficiency. The efficiency of the Chl-to-Car triplet transfer appears to be less than 100%. The Chl triplets for aggregates cannot be attributed to unbound Chl since no pigments were observed in the supernatant after spinning down the large aggregates in a sample without detergent. Also the fluorescence kinetics of macroaggregates have no decay components with a nanosecond lifetime contribution from free Chl (Barzda et al., unpublished results). Since there is no detectable change in the triplet transfer efficiency from Chl to Car upon disaggregation, we have no indication that free Chl is being formed. It was reported previously that at room temperature 100% of the Chl triplets are transferred to Car (6). Lower transfer efficiency of Chl triplets to Car in our measurements is possibly due to a better signal to noise ratio, although it should also be noted that LHCII was isolated in a different way in (6) and free Chl molecules were removed by purification on an anion exchange column in these preparations. However, this does not change the main conclusion that at room temperature very efficient transfer of Chl triplets to Car takes place (6). At low temperature, the triplet transfer efficiency from Chl to Car decreases to $82 \pm 6\%$, as observed before (6). The Chl's which are not transferring their triplets to Car probably do not have such a close contact with a Car as the other Chl's and at lower temperatures, a reduced probability of triplet transfer across the activation barrier results in a reduced transfer efficiency as compared to room temperature.

Upon disaggregation, Car's with their triplet absorption at 525 nm become relatively less populated as compared to the Car's with their triplet absorption at 508 nm. This can occur due to a reduction of the number of contacts between Chl's and Car's in neighboring trimers as was speculated in (14).

Effect of Disaggregation on Car-Chl Interactions. The main difference between the Car T-S spectra at room

temperature and 5 K (Figures 1 and 4A) is the change in the ratio of the signals at 506 and 678 nm. The ratio is equal to 5 at 5 K and remains unchanged upon disaggregation. In contrast, at room temperature the ratio is 8 for macroaggregates and remains almost unchanged for small aggregates. At the CMC, the ratio increases to 13 for trimers. The T-S signals in the red region (650–700 nm) decaying with the same lifetime as the Car signals have been observed before with laser flash photolysis and most likely arise from a change in interaction between Car and Chl when the Car is in its triplet excited state (6). ADMR- and FDMR-detected T-S signals with the microwave absorption frequency of Car's were also detected in the red region (15, 18). These changes show that different Car's have interactions with different Chl *a* molecules and that the interactions are affected upon disaggregation, although the triplet transfer efficiency remains basically unchanged. The Car-Chl interaction could be changed upon disaggregation through alteration of the protein conformation, e.g., the binding pocket of the pigment, or the breaking of specific intertrimer contacts. At low temperatures, the detergent effect is less pronounced.

CONCLUSIONS

In this work, we continued studies on the influence of aggregation on the excitation energy relaxation pathways in LHCII. Here we concentrated on the influence of aggregation on T-S spectra. From T-S and fluorescence yield measurements on LHCII at different aggregation states, we conclude the following:

1. Disaggregation leads to an increase of the triplet yield which appears to be due to a reduced quenching of the singlet excited states.
2. The radiative rate and the rate of intersystem crossing are not altered upon disaggregation.
3. The efficiency of triplet transfer in LHCII aggregates from Chl to Car is $92 \pm 7\%$ at room temperature and $82 \pm 6\%$ at 5 K, and does not decrease more than 4% upon disaggregation.
4. The Chl's that do not transfer their triplets appear to be bound to LHCII and seem to be in contact with the other Chl's as far as singlet transfer is concerned.
5. Disaggregation of macroaggregates into small aggregates reduces the ratio of the Car triplets absorbing at 525 and 506 nm by 10%. This effect is most likely due to a decreased efficiency of intertrimer Chl-Car triplet transfer. The triplet relaxation rates remain constant.
6. Around the CMC, where small aggregates disassemble into trimers, the detergent changes the interactions between Chl and Car. At room temperature, this leads to spectral changes in the Chl Q_y region which are caused by interactions between Chl and Car molecules.
7. The aggregation-dependent variations in the triplet population efficiency and decay rates appear to be small compared to the changes in the triplet yield due to aggregation-dependent quenching of singlet excited states.

ACKNOWLEDGMENT

We thank Dr. Ivo van Stokkum for help with the global analysis of the data and F. Calkoen for assistance with the sample preparations.

REFERENCES

1. van Grondelle, R., Dekker, J. P., Gillbro, T., and Sundström, V. (1994) *Biochim. Biophys. Acta* 1187, 1–66.
2. Kühlbrandt, W., Wang, D. N., and Fujiyoshi, Y. (1994) *Nature* 367, 614–621.
3. Siefermann-Harms, D. (1987) *Physiol. Plant.* 69, 561–568.
4. Hobe, S., Prytulla, S., Kühlbrandt, W., and Paulsen, H. (1994) *EMBO J.* 13, 3423–3429.
5. Jansson, S. (1994) *Biochim. Biophys. Acta* 1204, 1–19.
6. Peterman, E. J. G., Dukker, F. M., van Grondelle, R., and van Amerongen, H. (1995) *Biophys. J.* 69, 2670–2678.
7. Mullet, J. E., and Arntzen, C. J. (1980) *Biochim. Biophys. Acta* 589, 100–117.
8. Burke, J. J., Ditto, C. L., and Arntzen, C. J. (1978) *Arch. Biochem. Biophys.* 207, 252–263.
9. Simidjiev, I., Barzda, V., Mustardy, L., and Garab, G. (1997) *Anal. Biochem.* 250, 169–175.
10. Garab, G., Faludi-Dániel, A., Sutherland, J. C., and Hind, G. (1988) *Biochemistry* 27, 2425–2430.
11. Barzda, V., Mustardy, L., and Garab, G. (1994) *Biochemistry* 33, 10837–10841.
12. Barzda, V., Garab, G., Gulbinas, V., and Valkunas, L. (1995) in *Photosynthesis: from Light to Biosphere* (Mathis, P., Ed.) Vol. I, pp 319–322, Kluwer Academic Publishers, The Netherlands.
13. Ruban, A. V., Calkoen, F., Kwa, S. L. S., van Grondelle, R., Horton, P., and Dekker, J. P. (1997) *Biochim. Biophys. Acta* 1321, 61–70.
14. van der Vos, R., Franken, E. M., and Hoff, A. J. (1994) *Biochim. Biophys. Acta* 1208, 243–250.
15. Carbonera, D., Giacometti, G., and Agostini, G. (1992) *Appl. Magn. Reson.* 3, 859–872.
16. Nechushtai, R., Thornber, J. P., Patterson, L. K., Fessenden, R. W., and Levanon, H. (1988) *J. Phys. Chem.* 92, 1165–1168.
17. Carbonera, D., Giacometti, G., Agostini, G., and Toffoletti, A. (1989) *Gazz. Chim. Ital.* 119, 225–228.
18. van der Vos, R., Carbonera, D., and Hoff, A. J. (1991) *Appl. Magn. Reson.* 2, 179–202.
19. Carbonera, D., and Giacometti, G. (1992) *Rend. Fis. Acc. Lincei* 3, 361–368.
20. van Mourik, F., van der Oord, J. R., Visscher, K. J., Parkes-Loach, P. S., Loach, P. A., Visschers, R. W., and van Grondelle, R. (1991) *Biochim. Biophys. Acta* 1059, 111–119.
21. van Stokkum, I. H. M., Scherer, T., Brouwer, A. M., and Verhoeven, J. W. (1994) *J. Phys. Chem.* 98, 852–866.
22. Barzda, V., Garab, G., Gulbinas, V., and Valkunas, L. (1996) *Biochim. Biophys. Acta* 1273, 231–236.
23. Groot, M. L., Peterman, E. J. G., van Kan, P. J. M., van Stokkum, I. H. M., Dekker, J. P., and van Grondelle, R. (1994) *Biophys. J.* 67, 318–330.
24. Peterman, E. J. G., Gradinaru, C. C., Calkoen, F., Borst, J. C., van Grondelle, R., and van Amerongen, H. (1997) *Biochemistry* 36, 12208–12215.

BI972123A